JOURNAL OF MATERIALS SCIENCE 27 (1992) 1842–1848

Optical properties of polycrystalline and amorphous $Ni_{1-x}P_x$ layers by ellipsometry

A. A. WRONKOWSKA, A. WRONKOWSKI
Institute of Mathematics and Physics, Academy of Technology and Agriculture, Aleja S. Kaliskiego 7, 85-790 Bydgoszcz, Poland

The optical properties of polycrystalline and amorphous d.c.-electrodeposited $Ni_{1-x}P_x$ alloys in the visible spectral range are reported. Spectroscopic ellipsometry measurements of the pseudo-optical constants were performed from 1.65 to 3.1 eV for specimens with atomic fraction of phosphorus of $0.06 < x < 0.28$. It was found that the dielectric functions of as-deposited $Ni_{1-x}P_x$ could be expressed in the modified Drude-like form, including separate contributions from the interband transitions. Estimated values of the plasmon energy in the range of 5.3–3.1 eV and scattering time of the order of 10^{-15} s seem to show quantitative validity. A decrease in plasma frequency by a factor of about 1.4 across the glass-forming range agrees well with the predicted decrease in the s–p density of states at the Fermi level. Transformation of the amorphous $Ni_{0.725}P_{0.275}$ to the crystalline Ni_3P + Ni phase caused by heating results in changed optical functions which exhibit large deviation from the single nearly-free-carrier approach. This would suggest a two-carrier and/or frequency-dependent Drude parameters model as offering a more reasonable description of the optical conductivity of crystalline two-phase Ni–P systems.

1. Introduction

During the last 15 years, considerable interest has been focused on the properties of transition metal–metalloid alloys in the crystalline and amorphous states [1, 2]. Since nickel–phosphorus alloys exhibit not only interesting physical properties but also the possibility of technological applications (thin film resistors and underlayers of thin film magnetic discs), they have been extensively studied by different methods [3–13]. Various investigations have shown that the physical behaviour of Ni–P alloys, being dependent on P concentration, is strongly influenced by their structure [6–9, 14, 15] and less by the technique of preparation [7–9, 14].

In general, as-prepared $Ni_{1-x}P_x$ alloys with low P concentration, $x < 0.11$, are metastable supersaturated solid solutions of phosphorus in the microcrystalline f c c–Ni structure [8]. With increased phosphorus, the dimensions of the crystallites decrease from ~ 20 to a few nanometres [16] and amorphization takes place. However, controversy still exists in the literature as to whether the structure of P-rich alloys is amorphous or microcrystalline [16]. The amorphous state, in the sense that X-ray diffraction no longer indicates the existence of crystallites, can be achieved for samples with P concentration in very limited range, $0.15 < x < 0.3$. Amorphous Ni–P alloys are not stable, and under subsequent annealing transform into several crystalline phases (Ni_3P, $Ni_{12}P_5$, Ni) [8, 15].

Our knowledge of the electronic structure of transition-metal alloys is still in a rudimentary stage compared to that of pure metals. It is also not known in detail whether amorphization alters the electronic spectra of alloys with respect to the crystalline systems. The earlier works suggest that the stability of an amorphous alloy is essentially governed by the electronic density of states in the vicinity of the Fermi level [17, 18]. Most papers reporting on the optical, magnetic, catalytic and transport properties of Ni–P alloys relate the addition of P atoms to a charge transfer from P to Ni or from Ni to P [11, 13, 19–22]. Recent studies on the metal–metalloid amorphous alloys stress the problem of the existence of some short-range order (SRO) around the metalloid atoms [1, 19, 23, 24]. The SRO around transition-metal atoms was found to be looser than around s–p elements, which in nonstoichiometric amorphous alloys can lead to phase separation [25]. To our knowledge, no band-structure calculations for P concentrations $0 < x < 0.15$ are actually available.

The theoretical model of the optical conductivity in amorphous metals is very complex, and a complete description including multiple-scattering effects has not been presented as yet. Thus, in particular, a nearly-free-electron treatment with a single-scattering approximation can play the role of a first approach and explain many of the transport phenomena. However, little work has been done on the optical properties of $Ni_{1-x}P_x$ alloys. Until now the optical properties of Ni–P have been studied by reflectivity measurements [11, 13] in a narrow P concentration range only. The Drude-like behaviour of reflectivity spectra was observed for low frequencies [13].

The aim of this work was to get information concerning the optical properties of d.c.-electrodeposited $Ni_{1-x}P_x$ alloys in the concentration range of

0022–2461

$0.06 \leqslant x \leqslant 0.28$ including two types of structural transition: the first, from the crystalline to the amorphous state due to successive incorporation of a greater amount of P atoms; and the second, recrystallization by heating the amorphous P-rich specimen. The measurements were performed in the visible spectral range by means of spectroscopic ellipsometry. This means in practice that both the real, ε_1, and imaginary, ε_2, parts of the complex dielectric function $\tilde{\varepsilon} = \varepsilon_1 + i\varepsilon_2$ of bulk materials can be measured directly on a wavelength-by-wavelength basis without the need of Kramers–Kronig transformations or combinations of reflectance and transmittance measurements at different states of polarization and/or angles of incidence. Our previous investigations [26] of thick Ni–P coatings indicate that the optical constants and dielectric spectra measured with the use of visible light can probe the electronic properties of these alloys.

2. Experimental procedure

2.1. Sample preparation and characterization

The $Ni_{1-x}P_x$ coatings of different P concentration ($0.06 \leqslant x \leqslant 0.28$) and thickness of about 20–30 μm were prepared on brass substrates by d.c.-electrodeposition using bath conditions as in Brenner *et al.* [27]. The pH of the plating solutions was kept constant at 1, and temperature was maintained at 343 K. The direct current density applied was 0.5–1.0 nm dm^{-2}. No surfactants were added.

The bulk composition of the samples was determined by chemical techniques (the so-called molybdophosphoric method). For several Ni–P specimens, the atomic concentrations in the near-surface layers were verified by the Auger electron spectroscopy (AES) depth profile method. Some differences exist between the composition estimated from the chemical analysis and the AES data ($\sim \pm 0.01$). This may originate from the not exactly uniform spatial distributions of Ni and P atoms which are probably caused by local disturbances in the plating conditions. To check the crystalline and/or amorphous structure of the Ni–P alloys, X-ray diffraction scans were taken using CuK_α radiation as the X-ray source.

The crystallization of amorphous $Ni_{0.725}P_{0.275}$ specimens was performed in vacuum at a pressure of about 5 mPa by 1 h annealing at a temperature of about 950 K.

Just before optical measurements were taken, the samples were mechanically polished with alumina grit of grain size < 0.25 μm, washed in an ultrasonic bath and dried in an argon atmosphere.

2.2. Ellipsometric measurements

The pseudo-optical constants of the $Ni_{1-x}P_x$ alloys have been determined in the visible spectral range (1.65–3.1 eV) by means of spectroscopic ellipsometry. The measurements were performed at room temperature and under laboratory air conditions at intervals of $\delta\lambda = 10$ nm. The ellipsometer used was a static type equipped with a monochromator and Xe lamp (or He–Ne laser) as the light source. A regulated retarder was employed as compensator. The experimental errors of ellipsometric parameters Ψ and Δ, determined in two zones at an angle of incidence $\varphi = 70°$ are estimated to be $\pm 0.1°$ and $\pm 0.2°$, respectively. The complex pseudo-dielectric functions $\tilde{\varepsilon}(\omega) = \varepsilon_1(\omega) + i\varepsilon_2(\omega)$ were obtained from ellipsometric parameters using the well-known relation

$$\tilde{\varepsilon}(\omega) = \sin^2\varphi + [(1 - \tilde{r})^2/(1 + \tilde{r})^2]\sin^2\varphi\tan^2\varphi \quad (1)$$

where

$$\tilde{r} = tg\Psi \cdot e^{i\Delta} \quad (2)$$

represents the main equation of ellipsometry.

3. Results and discussion

3.1. Structure of $Ni_{1-x}P_x$ layers

The X-ray diffraction (XRD) patterns of as-deposited Ni–P alloy coatings are shown in Fig. 1. The spectra presented are computer separated from the joint Ni–P and substrate XRD patterns. Two peaks due to Miller indices (1 1 1) and (2 0 0) of Ni f c c structure appear at $\theta = 22.3°$ and 26°, respectively. Their positions are independent of the composition of samples within the experimental error. Any lines associated with the presence of Ni–P compounds were not revealed. The alloys with P concentration close to $x = 0.13$ show a broadening of the Ni (1 1 1) strong band, while the second maximum disappears. Specimens having $x > 0.2$ are completely amorphous. The sample with a P concentration of $x = 0.17$ exhibits a diffraction maximum higher than that of $x = 0.145$. This may imply that the former sample has a mixed structure composed of an amorphous phase and crystalline nickel precipitations, and the crystalline order dominates. Many experiments on $Ni_{1-x}P_x$ alloys show that total amorphization occurs only when P concentration reaches eutectic ($x \approx 0.19$) and that, at lower concentration, amorphous and disordered crystalline regions coexist [9, 16].

For $Ni_{0.725}P_{0.275}$ specimens, the crystalline structure appears after annealing (Fig. 2). The new maxima

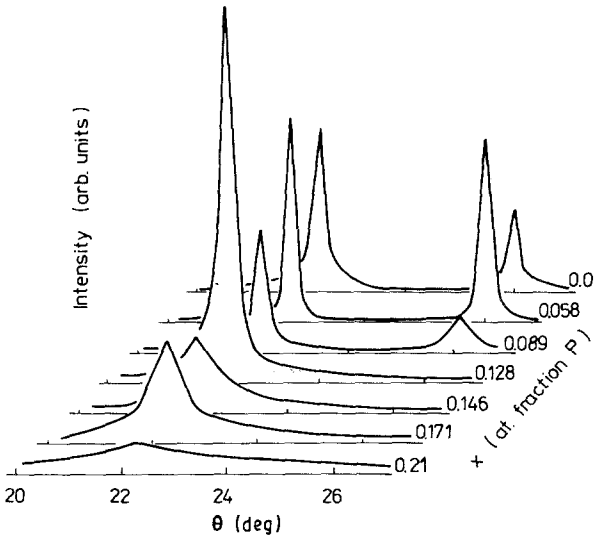

Figure 1 Computer-aided XRD patterns of as-deposited Ni and $Ni_{1-x}P_x$ layers.

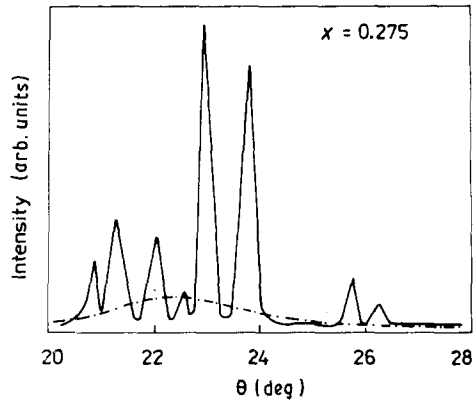

Figure 2 Computer-aided XRD patterns of (—·—) as-deposited and (——) annealed $Ni_{0.725}P_{0.275}$ alloys.

which appear on X-ray diffractograms of the annealed Ni–P alloy may correspond to the precipitated crystalline phase of Ni_3P [14, 15].

3.2. Optical data and analysis

The optical properties of homogeneous systems are completely characterized by complex dielectric functions. In the case of a heterogeneous material, however, an effective dielectric function can be attributed to the system if the wavelength of light is much larger than the typical size of the inhomogeneities.

The effects of P concentration and the structure of Ni–P alloy coatings on their optical properties are shown in Figs 3 and 4. The pseudo-optical constants of $Ni_{1-x}P_x$ specimens determined at $\lambda = 632.8$ nm (Fig. 3) reveal, in general, a decrease of extinction coefficient, k, with an increase in P concentration. This implies worse conductivity conditions with the increase of atomic fraction of P in the alloy. Larger differences in the extinction coefficients for samples with P concentration close to $x = 0.15$ reflect, most probably, the structure effect on optical properties of alloys and/or differences in spatial concentration of P atoms. The refractive index, n, remains practically constant up to $x = 0.15$. In the concentration region of mixed phases one can note a little jump of n to larger

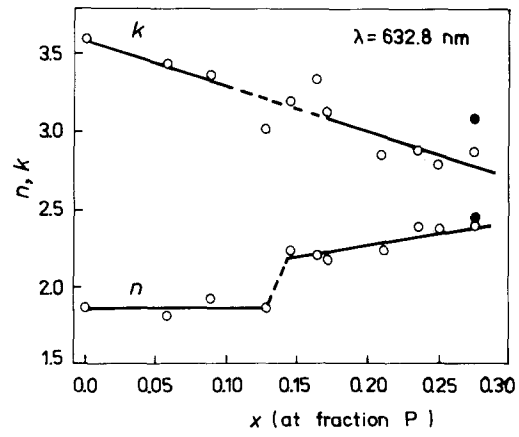

Figure 3 Pseudo-optical constants ($\tilde{n} = n - ik$) of $Ni_{1-x}P_x$ alloys, P concentration at $\lambda = 632.8$ nm. Open circles, as-deposited specimens; dark circles, annealed $Ni_{0.725}P_{0.275}$.

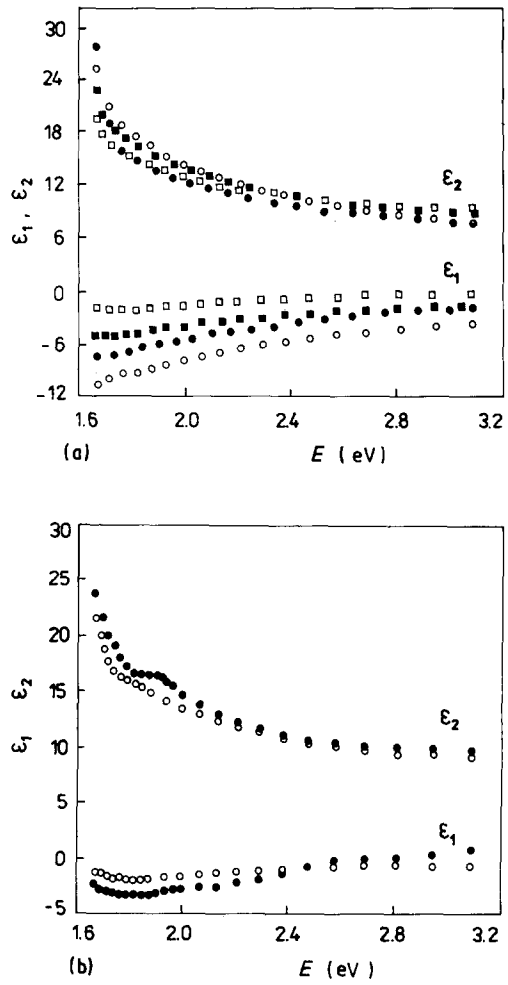

Figure 4 Real, ε_1, and imaginary, ε_2, parts of pseudo-dielectric function against $\hbar\omega$ for $Ni_{1-x}P_x$. (a) As-deposited specimen, x = ○, 0.058; ●, 0.128; ■, 0.171; □, 0.210. (b) As-deposited (open circles) and annealed (dark circles) $Ni_{0.725}P_{0.275}$.

values followed by a slow increase with an increasing amount of P atoms.

In the case of crystalline (annealed) $Ni_{0.725}P_{0.275}$ alloy, the refractive index is only slightly increased, whereas the extinction coefficient is evidently shifted to larger values. The AES spectra displayed an increased concentration of P in the near surface layers of recrystallized Ni–P specimens compared to that of their amorphous counterparts. However, the increased extinction coefficient of the annealed alloys for longer wavelengths of light cannot be explained, for the reasons mentioned above, as an effect of segregation of metalloid to the surface.

In Fig. 4 the real, ε_1, and imaginary, ε_2, parts of the pseudo-dielectric function of as-deposited $Ni_{1-x}P_x$ alloys and the annealed $Ni_{0.725}P_{0.275}$ specimen are plotted. The spectral variations of $\tilde{\varepsilon}$ are similar for as-deposited alloys in the microcrystalline ($x < 0.13$), mixed-phase ($0.13 < x < 0.20$) and amorphous ($x > 0.20$) states. With an increasing amount of P atoms, values of ε_1 considerably increase and both $\varepsilon_1(\omega)$ and $\varepsilon_2(\omega)$ functions show evident flattening. Larger differences, as a feature in $\varepsilon_2(\omega)$ below 2 eV, appear for annealed $Ni_{0.725}P_{0.275}$ samples (Fig. 4b).

The linear dependence of $-\varepsilon_1$ on ω^{-2} depicted in a wide range of light spectra (Fig. 5) encourages us to

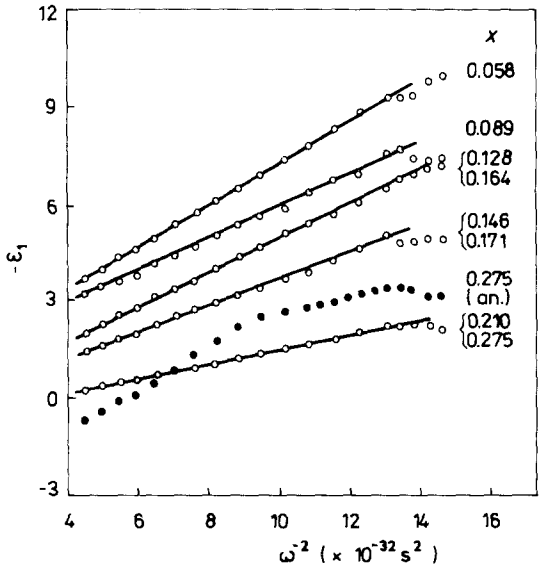

Figure 5 Real parts of pseudo-dielectric functions, $-\varepsilon_1$, against ω^{-2} for as-deposited $Ni_{1-x}P_x$ layers (open circles) and annealed $Ni_{0.725}P_{0.275}$ (dark circles). Solid lines are the least-squares fits to experimental data.

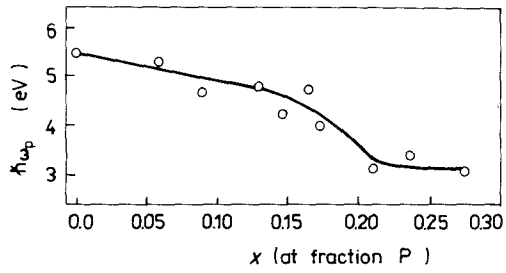

Figure 6 Effective plasmon energy, $\hbar\omega_p$, against P concentration. The solid line is drawn only to guide the eye.

presume that the pseudo-dielectric functions of as-deposited microcrystalline and amorphous $Ni_{1-x}P_x$ can be expressed in the Drude-like form, including separate contributions from the interband transitions emphasized in this spectral range. It is well known that transition metals are not formally free-electron-like systems, and both intraband and interband processes contribute to the dielectric function at lower energies of several tenths of eV [28]. The optical properties in the interband region are mainly determined by electronic transitions dependent on the local order. The influence of intraband contributions is generally larger in ε_1, as was observed for Ni [29]. Thus we assume that for visible light, the components of the complex dielectric function of approximately single phase Ni–P alloys can be described as a superposition of intraband (Drude formula) and interband transitions

$$\varepsilon_1(\omega) = \varepsilon_{1\infty} + \varepsilon_1'(\omega) - \omega_p^2/(\omega^2 + \gamma^2) \quad (3)$$

and

$$\omega\varepsilon_2(\omega) = 4\pi\sigma'(\omega) + \omega_p^2\gamma/(\omega^2 + \gamma^2) \quad (4)$$

where $\gamma = \tau^{-1}$ is the damping parameter, $\omega_p = (4\pi Ne^2 m_{op}^{-1})^{1/2}$ defines the plasma frequency, $\sigma'(\omega)$ and $\varepsilon_1'(\omega)$ represent the interband conductivity and the interband contribution to ε_1, respectively, and $\varepsilon_{1\infty}$ is the contribution from transitions at higher energies. If the interband contributions are less dispersive than intraband parts of $\tilde{\varepsilon}$ and $\omega\tau \gg 1$ is fulfilled, it is easy to extract $\varepsilon^\circ = \varepsilon_{1\infty} + \varepsilon_1'$ and ω_p by a linear least-squares fit of formula $-\varepsilon_1(\omega^{-2})$ obtained from Equation 3 applied to experimental data. The second Drude parameter, γ, and the interband conductivity, σ', can also be derived from Equations 3 and 4.

Other difficulties arise in the modelling of mixed-phase alloys, $0.1 < x < 0.2$. The systems can be represented as inhomogeneous mixtures, whose optical properties (effective) will depend on the volume fraction of amorphous clusters in a disordered matrix or on the volume fraction of microcrystalline metal-rich impurities in the amorphous matrix. Because their $\varepsilon_1(\omega^{-2})$ functions also follow a Drude law in this range (Fig. 5), we assume that the mixed-phase alloy dielectric function can also be approximated by a modified Drude function, with effective $\langle\omega_p\rangle$ and $\langle\tau\rangle$ parameters.

Fig. 6 demonstrates the dependence of the plasmon energy $\hbar\omega_p$, estimated from the slope of the linear part of $-\varepsilon_1(\omega^{-2})$ curves, as a function of the P concentration of as-deposited Ni–P alloys. For comparison, we have found $\hbar\omega_p$ for d.c.-electrodeposited pure Ni layers. Our value of the plasmon energy $\hbar\omega_p = 5.47 \pm 0.15$ eV, taken without correction for surface roughness and thin oxide layer, is in agreement with the results reported by Lynch *et al.* [28] and Gadenne and Lavait [30] of 5.23 and 5.74 eV, respectively. It is rather difficult to ascertain the effect of the surface structure on dielectric function. We assume that under the preparation conditions, the influence of the surface roughness and the thickness ($\sim$ 1 nm) of the oxide layer is similar for all samples. This may result in a small increase of $\varepsilon_1(\omega)$ and decrease of $\varepsilon_2(\omega)$ without a substantial change in the shape of the dielectric spectra. The spectral form of pseudo-dielectric data of the anodically oxidized $Ni_{0.725}P_{0.275}$ surface (covered with an $\sim$ 5-nm-thick passive layer) confirms these assumptions. Consequently, the presence of the thick oxide layer considerably alters ε° but the slope of the $-\varepsilon_1(\omega^{-2})$ line remains unchanged, giving the same value of ω_p.

The presence of P atoms in the microcrystalline Ni matrix of low P content ($x < 0.10$) Ni–P alloys does not have much influence on the estimated values of plasmon energy. A considerable decrease of $\hbar\omega_p$ with the increase of x above 0.145 can be explained by the decrease in the effective number of nearly-free carriers with increased P concentration. Such a dependence is consistent with the density of states calculations of Khanna *et al.* [21] and Ching [20]. These authors point out the minimum s–p density of states at the Fermi level for amorphous Ni–P alloys. Khanna *et al.* [21] show that the density of states at the Fermi level (which is essentially unchanged) decreases by a factor of 1.4 within the metalloid atomic fraction range 0.15–0.26. Our decreasing factor of 1.9 taken from $[\omega_p(0.15)/\omega_p(0.275)]^2$ is also comparable to a corresponding decrease by a factor of 2.3 deduced from the specific heat measurements, and a decrease by a factor of 1.6 derived from the Knight-shift experiments known from the literature [6, 12]. Similar behaviour

of plasma frequency for amorphous Ni–P layers was reported earlier by McKnight and Ibrahim [13] from a computer fitting of i.r.-reflectivity spectra. Although their values of $\hbar\omega_p$ of about 17 eV at low P concentration (15 at %), and a corresponding decrease of nearly-free carriers by a factor of about 5 across the glass-forming range, seem to be rather large.

Values of the electron scattering time, $\tau = \gamma^{-1}$, were extracted from the plots of $\omega\varepsilon_2/[\varepsilon^\circ - (n^2 - k^2)]$ against ω^2 which exhibit linear dependence in the large part of the spectra, and by a fit of $\varepsilon_1(\omega)$ to experimental data using previously estimated values of ω_p and ε°. The results also confirm the dependence of $\langle\tau\rangle$ on P concentration, but the relationship between $\langle\tau\rangle$ and x is more complex as can be seen from Fig. 7. For microcrystalline alloys ($x < 0.13$) we observe a decrease in scattering time from about 9×10^{-15} s for $x = 0.058$, down to about 2×10^{-15} s for $x = 0.13$. One might expect the electron-scattering time for low atomic fraction of $Ni_{1-x}P_x$ samples would not differ much from that determined for pure Ni. The relaxation times of Ni deduced with the help of different methods are in the range of 1.1–1.3 $\times 10^{-14}$ s [28, 30, 31]. This means that our effective relaxation times are shorter by a factor of 1.3–5.0 for x ranging from 0.06 to 0.13. Amorphous specimens demonstrate a slight tendency to increase the carrier-scattering time with an increasing number of P atoms, from 2×10^{-15} to 3×10^{-15} s in the concentration range of $0.15 < x < 0.275$. Such τ variations for amorphous Ni–P alloys were also found by McKnight and Ibrahim [13] and this corresponds well with the s–p density of states calculations [20, 21]. This also indicates that the electron-scattering process is dominated mainly by the added metalloid impurities and less by the displacement of Ni atoms [32]. Our values of τ within the order of magnitude of 10^{-15} s seem to be realistic; however, the results must be considered with caution, since estimation of τ is not strictly independent and errors are possible.

It is noteworthy that calculated values of the optical resistivity at $\omega = 0$, $\rho_{op} = 4\pi/\omega_p^2\tau$, using our values of $\langle\omega_p\rangle$ and $\langle\tau\rangle$, range from about 20 $\mu\Omega$ cm for $x = 0.058$ up to about 180 $\mu\Omega$ cm for $x = 0.275$, and are in very good agreement with d.c.-resistivities of Ni–P alloys known from the literature [9, 10, 14, 32]. We thus conclude that the increased resistivity of as-deposited low P concentration Ni–P systems is due to both an increase of effective scattering rate, and a decrease in plasma frequency. The increased resistivity of amorphous specimens with larger P concentration is due only to decreased plasma frequency.

The real part of the complex total optical conductivity spectra, $\sigma = \omega\varepsilon_2/4\pi$, depends on P concentration being less dependent on frequency for samples in the amorphous state (Fig. 8a). The curves for samples with P concentrations of $x = 0.21$, 0.24 and 0.275 differ only a little. Larger values of σ for amorphous alloys than for low P concentration specimens in the higher frequency part of the spectrum appear to be consistent with the prediction derived by Ching [20] from the joint density of states calculations. In Fig. 8b we demonstrate the interband optical conductivity spectra σ' (multiplied by $\hbar$) obtained for as-deposited Ni–P alloys from $\omega\varepsilon_2$ spectra after subtraction of the Drude contribution. One can see from Fig. 8 that the structure of the optical conductivity is affected not only by the concentration of P atoms but also by the structure of the samples. The contribution of the Drude-like free carriers to the optical conductivity is, in general, very small.

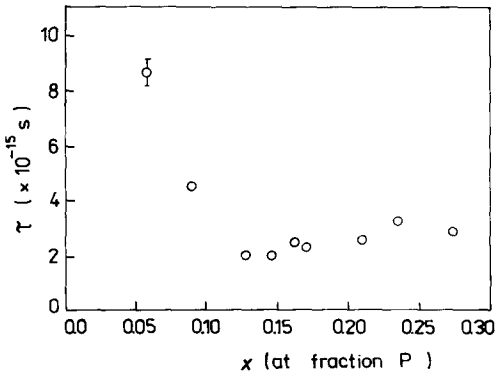

Figure 7 Effective scattering time against phosphorus concentration estimated for as-deposited $Ni_{1-x}P_x$ alloys.

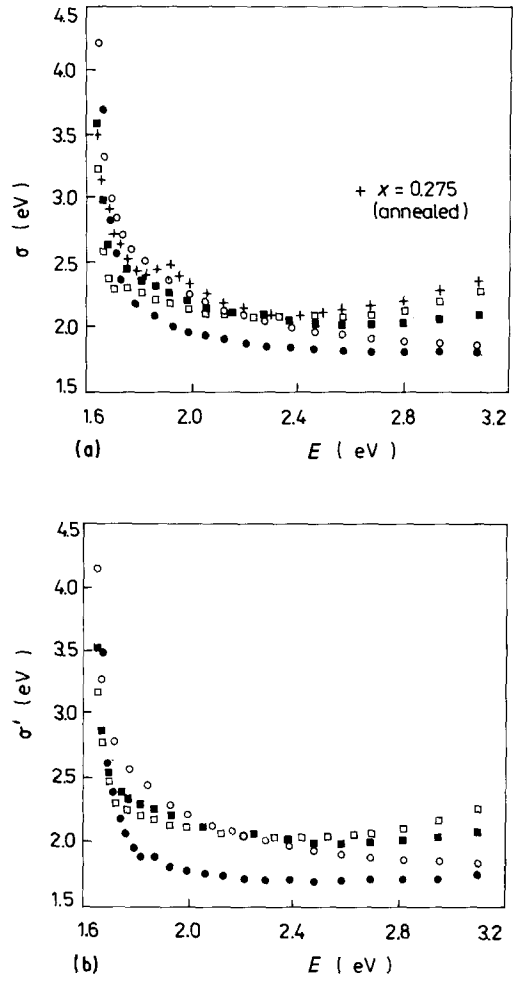

Figure 8 (a) Real part of the total optical conductivity, σ (in eV); (b) interband conductivity σ' against $\hbar\omega$ for as-deposited microcrystalline and amorphous $Ni_{1-x}P_x$ alloys. x = ○, 0.058; ●, 0.128; ■, 0.171; □, 0.275; and +, 0.275 (annealed).

Major differences between amorphous and crystalline $Ni_{0.725}P_{0.275}$ optical conductivity spectra (Fig. 8a), like larger values of σ and a small peak for the latter specimens, are manifested in the low-energy part of the reported spectra. These may confirm that the interband transitions play an intrinsic role in this spectral range. A similar structure of σ spectra, located between 1.4 and 1.7 eV, has also been observed for Ni samples [30, 33, 34] and is established to be dependent on crystallite size: the smaller the crystallites, the weaker the structure. This explains a weak structure of σ' (interband conductivity) spectra observed for as-deposited low P concentration (microcrystalline) samples. Large deviation from the single carrier Drude-like approach seen in Fig. 5 may suggest two-carrier and/or frequency-dependent ω_p and τ models for recrystallized P-rich Ni–P alloys. The observed effect is not surprising. The heterogeneous conductor, consisting of well-defined constituents (such as crystalline Ni_3P and Ni) with different electronic properties, can be approximated by an effective medium (Maxwell–Garnett or Bruggeman theory, for example) whose properties are a function of the conductivity of each medium and of the volume fraction of one medium in relation to the other [32, 35]. Because of a narrow energy range and probable predominant interband contributions, we have not been able to demonstrate a realistic description of optical conductivity within a two-carrier effective medium model for a recrystallized P-rich Ni–P alloy. It should be noted that drastic changes of transport properties in $Ni_{0.76}P_{0.24}$ after heating above 600 K were reported earlier by Cote and Meisel [10]. Transformation of amorphous alloys to the crystalline Ni_3P + Ni phase resulted in a large reduction in electrical resistivity. This effect is consistent with changes in the optical properties of annealed Ni–P alloys.

4. Conclusions

The knowledge of optical properties of the system under consideration gives an insight into both electronic transport and electronic structure. Ellipsometry was employed with success to obtain reliable optical functions of the polycrystalline and amorphous $Ni_{1-x}P_x$ alloys over the visible spectral range. An approximate formula that allows a comparison of experimental data with the single-carrier model, including separate contributions from interband transitions, has been used. The simplified model of superposition of intraband and interband transitions gives a good description of the dielectric spectra of metastable Ni–P specimens, in the sense that we are able to extract the Drude parameters. We believe that our effective values of ω_p and τ describe, at least qualitatively, the electronic properties of $Ni_{1-x}P_x$ alloys for x not larger than 0.3. Plasmon energies of 5.3–3.1 eV for x ranging from 0.06 to 0.27, and a scattering time of the order of 10^{-15} s, seem to be realistic. The decrease in plasma frequency by a factor of about 1.4 across the glass-forming range is consistent with Khanna *et al.*'s [21] calculations of the density of states for amorphous Ni–P alloys, and predicts the decrease of the s–p density of states at E_f. The dependence of the plasma frequency and relaxation time on x can be related to the increase of d.c.-resistivity of Ni–P with an increased scattering rate and decreased plasma frequency.

Changes in the optical functions due to annealing of the $Ni_{0.725}P_{0.275}$ alloy suggest an application of a more sophisticated model, such as a two-carrier and/or frequency-dependent ω_p and τ approach, and an effective medium theory for the description of optical and electronic properties of crystalline P-rich Ni–P systems. To verify the validity of the models proposed here, further investigations extended to lower- and higher-frequency ranges are needed.

Acknowledgements

The authors wish to thank Dr S. Frackiewicz for preparation of the $Ni_{1-x}P_x$ coatings, Dr J. Owedyk for performing X-ray diffractograms, and Dr A. Bukaluk and Dr R. Siuda for AES analysis. Thanks are also due to Docent J. Skonieczny for helpful discussions and critical reading of the manuscript. This work was partly supported by the Polish Ministry of National Education within CPBP 01.08.

References

1. U. MIZUTANI, in "Progress in Material Science", Vol. 28, edited by J. W. Christian, P. Haasen and T. B. Massalski (Pergamon, Oxford, 1985) p. 97.
2. R. HASEGAWA (ed.), "Glassy Metals: Magnetic, Chemical and Structural Properties" (CRC Press, Boca Raton, Florida, 1983) Chs. 4 and 8.
3. A. SZASZ, J. KOJNOK, L. KERTESZ, Z. PAAL and Z. HEGEDUS, *Thin Solid Films* **116** (1984) 279.
4. W. A. HINES, C. U. MODZELEWSKI, R. N. PAOLINO and R. HASEGAZA, *Solid State Commun.* **39** (1981) 699.
5. L. MENDOZA-ZELIS, L. THOME, L. BROSSARD, J. CHAUMONT, K. KROLAS and H. BERNAS, *Phys. Rev. B* **26** (1982) 1306.
6. D. S. LASHMORE, L. H. BENNETT, H. E. SCHONE, P. GUSTAFSON and R. E. WATSON, *Phys. Rev. Lett.* **48** (1982) 1760.
7. I. BAKONYI, L. K. VARGA, A. LOVAS, E. TOTH-KADAR and A. SOLYOM, *J. Magn. Magn. Sci.* **50** (1985) 111.
8. U. PITTERMAN and S. RIPPER, *Phys. Status Solidi (a)* **93** (1986) 131.
9. L. THOME, A. TRAVERSE and H. BERNAS, *Phys. Rev. B* **28** (1983) 6523.
10. P. J. COTE and L. V. MEISEL, *Phys. Rev. B* **20** (1978) 20.
11. J. RIVORY, B. BOUCHET and Y. BERTRAND, *J. Physique* **41** (1980) C8-430.
12. Y. S. TYAN and L. E. TOTH, *J. Electron. Mater.* **3** (1974) 791.
13. S. W. McKNIGHT and A. K. IBRAHIM, *Phys. Rev. B* **29** (1984) 6570.
14. T. OSAKA, M. USUDA, I. KOIWA and H. SAWA, *Jpn J. Appl. Phys.* **27** (1988) 1885.
15. G.-X. LU, G. F. LI and F.-Ch. YU, *Wear* **103** (1985) 269.
16. G. DIETZ and H. D. SCHNEIDER, *J. Phys. Cond. Mater.* **2** (1990) 2169.
17. S. R. NAGEL and J. TAUC, *Phys. Lett.* **35** (1975) 380.
18. V. L. MORUZZI, P. OELHAFEN and A. R. WILLIAMS, *Phys. Rev. B* **27** (1983) 7194.
19. P. PANISSOD, I. BAKONYI and R. HASEGAWA, *ibid.* **28** (1983) 2374.
20. W. Y. CHING, *ibid.* **34** (1986) 2080.
21. S. N. KHANNA, A. K. IBRAHIM, S. W. McKNIGHT and A. BANSIL, *Solid State Commun.* **55** (1985) 223.

22. T. IMANAKA, in "Succesful Design of Catalysis", edited by T. Inui (Elsevier, Amsterdam, 1988) p. 3.
23. P. H. GASKELL, *J. Non-Cryst. Solids* **32** (1979) 207.
24. J. WONG and H. H. LIEBERMANN, *Phys. Rev. B* **27** (1984) 651.
25. M. R. PRESS, S. N. KHANNA and P. JENA, *ibid.* **36** (1987) 5446.
26. A. A. WRONKOWSKA and A. WRONKOWSKI, in Proceedings of the 2nd Polish Conference on Surface Physics, Vol. III, Wrocław, 1987 (Łódź University) p. 196.
27. A. BRENNER, D. E. CONCH and E. K. WILLIAMS, *J. Res. NBS* **44** (1950) 109; A. Brenner, "Electrodeposition of Alloys", Vol. 2 (Academic, New York, London, 1963).
28. D. W. LYNCH, R. ROSEI and J. H. WEAVER, *Solid State Commun.* **9** (1971) 195.
29. S. K. BOSE, L. E. BALLENTINE and J. E. HAMMERBERG, *J. Phys. F* **13** (1983) 2089.
30. M. GADENNE and J. LAVAIT, *J. Physique* **47** (1986) 1405.
31. A. P. LENHAM and D. M. TREHERNE, in "Optical Properties and Electronic Structure of Metals and Alloys", edited by F. Abeles (North-Holland, Amsterdam, 1966) p. 196.
32. A. TRAVERSE, E. PAUMIER, P. NEDELLEC, H. BERNAS, L. DUMOULIN and J. CHAUMONT, *Phys. Rev. B* **37** (1988) 2495.
33. B. Y. YANG, P. KLOSOWSKI, K. VEDAM and J. S. LANNIN, *ibid.* **38** (1988) 1562.
34. D. G. LAURENT, J. CALLAWAY and C. S. WANG, *ibid.* **20** (1979) 1134.
35. D. E. ASPNES, *Thin Solid Films* **89** (1982) 249.

Received 27 November 1990
and accepted 10 April 1991